文章编号：1001-9014(2022)02-0420-05
DOI:10. 11972/j. issn. 1001-9014. 2022. 02. 006

Preparation of epi-ready InAs substrate surface for InAs/GaSb superlattice infrared detectors grown by MOCVD

LIU Li-Jie[1*], ZHAO You-Wen[1,2], HUANG Yong[3], ZHAO Yu[3], WANG Jun[1], WANG Ying-Li[1], SHEN Gui-Ying[1], XIE Hui[1]

(1. Key Laboratory of Semiconductor Materials Science, Beijing Key Laboratory of Low Dimensional Semiconductor Materials and Devices, Institute of Semiconductors, Chinese Academy of Sciences, Beijing 100083, China;
2. College of Materials Science and Opto-electronic Technology, University of Chinese Academy of Sciences, Beijing 100049, China;
3. Key Lab of Nanodevices and Applications, Suzhou Institute of Nano-Tech and Nano-Bionics, Chinese Academy of Sciences, Suzhou 215123, China)

Abstract: Total reflection X-ray fluorescence spectroscopy (TXRF) and X-ray photo-electron spectroscopy (XPS) have been used to investigate residual impurities and oxides on polished InAs substrate surface wet cleaned by different solution combination. Metal impurities Si, K and Ca are routinely detected on the cleaned InAs surface and their concentration change with the variation of solution combination. A large quantity of particles (80 nm size) is measured on the InAs substrate surface with higher residual impurity concentration. An effective wet chemical cleaning procedure is presented to prepare InAs substrate surface with less residual impurity, small particle quantity and thin oxide layer, which are beneficial to high quality epitaxial growth.

Key words: InAs, substrate, surface cleaning, total reflection X-ray fluorescence (TXRF), X-ray photo-electron spectroscopy (XPS)
PACS: 81. 05Ea, 81. 65. cf, 91. 60. Ed, 81. 15. Gh

面向MOCVD生长InAs/GaSb超晶格红外探测的InAs衬底表面制备

刘丽杰[1*]，赵有文[1,2]，黄 勇[3]，赵 宇[3]，王 俊[1]，王应利[1]，沈桂英[1]，谢 辉[1]
(1. 中国科学院半导体研究所 材料重点实验室 北京市低维半导体材料与器件重点实验室，北京 100083；
2. 中国科学院大学 材料科学与光电技术学院，北京 100049；
3. 中国科学院苏州纳米技术与纳米仿生研究所 纳米器件与应用重点实验室，江苏 苏州 215123)

摘要：采用全反射X射线荧光光谱(total reflection X-ray fluorescence，TXRF)和X射线光电子能谱(X-ray photo-electron spectroscopy，XPS)检测方法研究InAs衬底化学机械抛光后经过不同湿法化学溶液联合作用后衬底表面的金属杂质残留浓度和氧化物组分的变化。湿法化学清洗后的InAs表面检测到金属杂质Si，K和Ca，它们的浓度随溶液组合的变化而变化。金属杂质残留浓度较高的InAs衬底表面同时也测得较多粒径为80 nm的颗粒。提出了一种行之有效的InAs衬底湿化学清洗方法，可制备出金属杂质残留少、颗粒少、氧化层薄InAs衬底表面，此表面有利于MOCVD方法生长高质量InAs/GaSb超晶格红外探测器外延。
关 键 词：砷化铟；衬底；表面清洗；全反射X射线荧光光谱；X射线光电子能谱
中图分类号：O43 **文献标识码**：A

Introduction

InAs is an important Ⅲ-Ⅴ semiconductors with narrow bandgap, high electron mobility and many applications in micro- and opto-electronic devices [1-2]. Especially, it is a useful substrate for InAs/GaSb Type-II superlat-

Received date: 2021-06-18, **revised date**: 2021-08-25 **收稿日期**：2021-06-18，**修回日期**：2021-08-25
Foundation items: Supported by National Natural Science Foundation of China (61904175)
Biography: LIU Li-Jie (1981-), female, Hebei China, Ph. D. Research on III-V semiconductor material character and defect
* **Corresponding author**: liulijie@semi. ac. cn

tice infrared detectors due to a lattice constant of 6.054 Å nearly match to GaSb with 6.094 Å [3-5]. Generally, high quality of epitaxial growth and device strongly requires a good cleaning technique to achieve high-quality epi-ready InAs substrate surface foundation. Researchers have employed many experiments and established reviews that the alkaline solutions are accompanied by the removal of the part of particle and then the formation of a thin chemical oxide from Si and GaAs exactly [6-7]. For InP substrate, alkaline solution basically was used as predominantly chemical treatments and originally designed for Si and GaAs, which possess similarity to the material characterization [8-9]. Also some reports which require the addition of an acidic solution show this is not the case due to the difference oxide behavior between indium and gallium [10]. For InAs substrate, Some researchers treated InAs surfaces with sodium sulfide aqueous solutions in order to removal a natural oxide layer [11], some used a combination of HF: methanol wet etching followed by atomic hydrogen treatment to achieve the result of oxide removal [12], and some studied the kinetic between HCl and InAs through a quantitative analysis of the oxide formation [13]. However, InAs epi-ready substrate prior to epitaxial growth through surface characteristics (i. e. particle, residual impurities and nature oxide thickness) has not been studied extensively.

In this work, NH_4OH, HCl and H_2O_2 based solutions were combined used with an aim to remove particle, residual impurities and leave a thin oxide layer on the substrate surface. Furthermore, an appropriate stoichiometric InAs surface were obtained in order to desorb easily during epitaxial growth process. With the help of TXRF, XPS, Scanning Electron Microscope (SEM) and surface scan measurement, an effective chemical cleaning procedure is presented for the preparation of high quality InAs epi-ready substrate.

1 Experimental

2-inch un-doped InAs wafers with (100)-orientation were sliced from an InAs (100) ingot grown in our laboratory by the liquid-encapsulated Czochralski (LEC) method [14-17]. The InAs wafers were lapped, polished, cleaned and packaged as epi-ready substrate in a class 100 cleaning room. During the final cleaning processing, different multi-step wet chemical cleaning processes were employed as listed in Table 1.

Three wet chemical cleaning processes were used to remove wafer contamination including particulate contamination, organic contamination and metallic contamination *et al*. Residual metal impurities on the wafer surface have been analyzed quantitatively by TXRF. The cleaned wafer surface defects, including particles, scratches, large pits, etc. were detected and classified using a KLA-Tencor Candela surface scanner. Nature oxide layer on the wafer surface was shown by an ellipsometer measurement. XPS is used to check oxide composition. Epitaxial defects morphology and formation are analyzed by SEM and Transmission electron microscopy (TEM), respectively.

2 Results and discussion

2.1 Residual metal impurities and particles

TXRF was used to detect and compare metal contamination on the wafer surface treated with different wet solutions. Table 2 demonstrate residual metal concentration on the InAs wafer surface cleaned with different solution combination.

NH_4OH: H_2O_2: H_2O based solution (SC1) are quite effective to remove particles and widely used in the wafer cleaning process of Si and GaAs substrates [6-7,10]. In this work, the solution (NH_4OH: H_2O_2: H_2O=1:1:10) is also proved to be effective in removing particles. In addition, metal impurities Ti, Cr, Mn, Fe, Ni, Cu, Zn on the InAs wafer is below the detection limitation. However, it is noted that alkali metals (K, Ca) and other elements (Si, S, Cl) remain at a very high concentration around 10^{14} atoms/cm^2 on the wafer surface (sample A). It is necessary to further reduce the concentration of alkali metals to avoid their negative influence on the electrical property of InAs based epitaxial layer and device performance [18]. Dilute HCl solution is used to dissolve the metals because the charge exchange reaction is followed by $M + 2H^+ \rightarrow M^+ + H_2O$, metals transfer to ions and removed by DI water rinse. As shown in Table 1, the concentration of residual alkali metal on the surface of sample B is significantly lower after the cleaning process.

Table 1 Multi-step wet cleaning processes used in this study
表1 各样品多步式清洗工艺

Sample No.	Wet Chemical Cleaning Step				
A			NH_4OH:H_2O_2:H_2O=1:1:10	Rinse	Dry
B	HC1:H_2O=1:30	Rinse	NH_4OH:H_2O_2:H_2O=1:1:10	Rinse	Dry
C	HC1:H_2O=1:30	Rinse	NH_4OH:H_2O_2:H_2O=1:0.2:10	Rinse	Dry

Table 2 TXRF results of the InAs wafer surface treated with different solution (10^{10} atoms/cm^2)
表2 不同溶液处理InAs衬底表面的TXRF结果(1010 atoms/cm2)

Sample No	Si	P	S	C1	K	Ca	Ti	Cr	Mn	Fe	Ni	Cu	Zn
A	1 051	0	428	1 057	44 542	7 553	0	0	0	0	0	0	0
B	494	0	244	544	38 129	3 711	0	0	0	1	0	0	0
C	197	0	77	478	38 130	3 164	0	0	0	0	0	0	0

Reduction of the H_2O_2 concentration in SC-1 by a factor of 5 has the effect to prevent micro-roughening of the InAs surface and to enhance metal particle removal. On the other hand, hydrogen peroxide in the solution has a higher oxidation potential and strong oxidation capacity. Compared with the high concentration of hydrogen peroxide in SC-1 solution, the lower solution possesses the weaker oxidability and the stronger complexation, therefore it is more conducive to the removal of metal ions. As a consequence, sample C has the lowest residual metal contamination among the three wafers treated by the different cleaning processes.

Figure 1 presents the KLA-Tencor Candela map metrology of particles on the InAs wafer treated by the three wet cleaning processes, respectively. Generally, the particle on the wafer has characteristic dimensions that can span several orders of magnitude, depending on the cleaning effect. For the three InAs wafer samples, most of the particles have size ranging from 0.08 μm to 0.15 μm (the detection limit of the instrument is 0.08 μm), as shown in the figure 1 labeled by green point. The total particle counts of the three sample wafers are 4428, 1243 and 875, respectively, with 3-mm edge exclusion. Refer to the results given in Table 2, the variation trend of particle quantity correlates well with metal contamination concentration. This is reasonable since the particle itself must be consisted of impurities.

2.2 Nature oxide stoichiometry and thickness

As an epi-ready substrate for high quality epitaxial growth, the residual oxides on the InAs is of considerable importance. The surface of indium arsenide has a large number of indium or arsenic suspension bonds with an unsaturated state after chemical mechanical polishing. The arsenic dangling bond prior to indium dangling bond combines with oxygen atoms from the InAs substrate, forming As_2O_3 on substrate surface that will continue to react with InAs single crystal surface through chemical Eqs. 1-2. This causes large amounts of indium trioxide adhere to the wafer surface. In_2O_3 can be dissolved from the wafer surface via chemical reaction in HCl solution as shown in Eq. 3. Besides, a low dose of H_2O_2 from SC-1 in the final process can stop the formation of the indium oxide due to chemical reaction given by Eq. 4-5 [19]. In this way, the thickness of the oxide on the wafer surface of sample C is quite small, as shown in the following results.

$$2As + 3O \rightarrow As_2O_3 \quad , \quad (1)$$

$$2InAs + As_2O_3 \rightarrow In_2O_3 + 4As \quad , \quad (2)$$

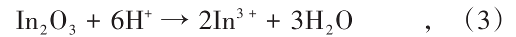

$$In_2O_3 + 6H^+ \rightarrow 2In^{3+} + 3H_2O \quad , \quad (3)$$

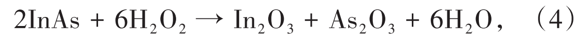

$$2InAs + 6H_2O_2 \rightarrow In_2O_3 + As_2O_3 + 6H_2O \quad , \quad (4)$$

$$InAs + 2H_2O_2 \rightarrow InAsO_4 + 2H_2O \quad . \quad (5)$$

Table 3 shows the results of five points native oxide thickness, including the center and 4 positions around the center by 1.5-cm. To check the oxides thickness, ellipsometer measurement is conducted to compare oxide thickness on the wafer surface undergone the multi-step wet chemical cleaning process [20]. The nature oxide layer thicknesses are 15.04Å, 10.19Å and 8.87Å, respectively. Sample B and sample C have lower native oxide thickness for HCl can dissolve the oxides effectively.

Table 3 Native oxide thickness measured by ellipsometer
表3 椭偏仪测量自然氧化层厚度

Sample	X/cm	Y/cm	Thickness/Å	Average/Å
Sample A	0	1.5	15.17	15.04
	1.5	0	15.01	
	0	0	14.93	
	-1.5	0	15.07	
	0	-1.5	15.01	
Sample A	0	1.5	10.27	10.19
	1.5	0	10.34	
	0	0	10.26	
	-1.5	0	9.90	
	0	-1.5	10.18	
Sample A	0	1.5	9	8.87
	1.5	0	8.9	
	0	0	8.79	
	-1.5	0	8.89	
	0	-1.5	8.78	

Moreover, a substrate wafer with stoichiometric thin oxide layer, less particle and low residual impurity concentration is highly high quality epi-growth. In order to

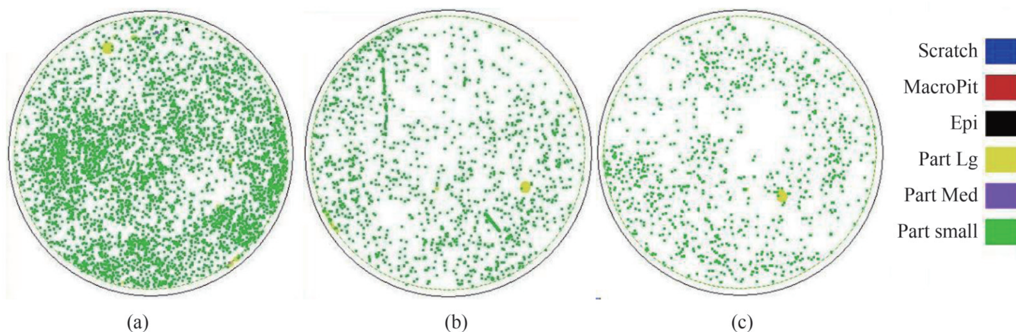

Fig. 1 KLA-Tencor Candela particle metrology maps of the three InAs wafer surface treated by different wet cleaning processes (a)sample A, (b)sample B, and (c)sample C
图1 三种不同湿法清洗工艺处理后KLA-Tencor颗粒度(a)样品A，(b)样品B，(c)样品C

clarify the chemical composition of oxides on the InAs wafer surface from sample B and sample C, XPS was used to analyze the core level and valence-band spectra of the oxides, as shown in Fig. 2. Binding energies and energy separation, for core levels, are presented in table 4. Due to charging effects, absolute binding energies are given with a deviation of ±0.3 eV[21]. By verifying the binding energy values some parameters can be determined for the identification of oxide composition.

From the measured results, it is able to distinguish the existed oxide from particular shapes of In3s and As3d spectra. Compounds In_2O_3, As, As_2O_3 and As_2O_5 were identified according to the specific binding energy. By calculating the peak intensity area ratio of indium and arsenic, the atomic ration of indium and arsenic are 0.8182 and 0.7061 for sample B and sample C, respectively. This result suggests that sample C has more arsenic rich oxide than sample B on its surface.

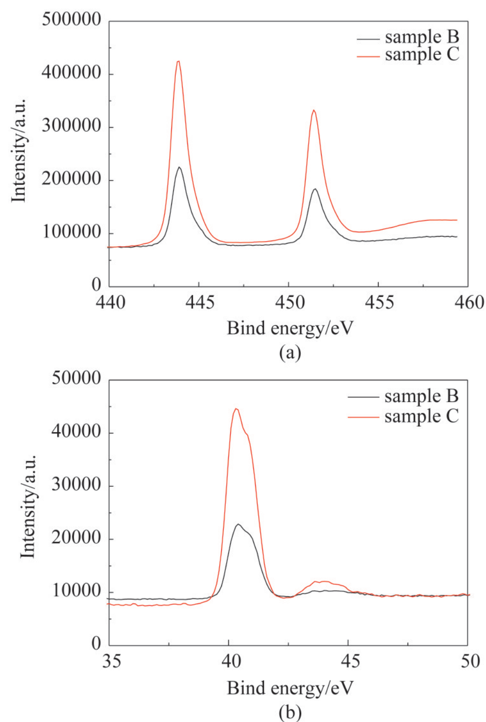

Fig. 2　XPS spectra of wafer B and C, details of the binding energy given in Table 4
图2　样品B和样品C的XPS能谱,结合能数据详见表4

Table 4　Binding energy of the peaks in XPS spectra and In/As Atomic percent of sample B and C
表4　样品B和样品C的XPS谱峰和In原子与As原子的百分比

Sample	In3d(eV)		As3d(eV)				In/As Atomic percent
	In_2O_3	InAs	In_2O_5	As_2O_3	As	InAs	
	451	444	45.2	44.5	41.6	40.5	
B	451.5	444.09	45.2	44.2	41.6	40.9	81.82%
C	451.4	443.93	45.1	44.1	41.3	40.6	70.61%

2.3　Epitaxial results

On the preparation InAs substrates of sample B and sample C, a 200 nm n+ LWSL bottom contact, an LWSL absorber of 2 μm thickness, a MWSL barrier of 200 nm and another 200 nm-thick p-MWSL contact were deposited in the same run by an Aixtron 2400G3 MOCVD growth system. Details on epitaxial design and growth are described in Ref. [22]. The defect density of epitaxial surface is observed by a Normarski (Fig. 3). The epitaxial defect density from sample B is 990/cm^2 (Fig. 3(a)), while 140/cm^2 is from sample C (Fig. 3(b)). The defect in morphology look like hillocks with about 9 μm×6 μm, which is obtained by a scanning electron microscopy analyses, as shown in Fig. 4. A TEM sample was prepared by using a focused ion beam. TEM (Fig. 5) showed that there was a bulge at the interface between substrate and epitaxial. This bulge forms the center of the defect source, causing epitaxial growth stress in the epitaxial layer. This little bump could be a particle, a residue metal impurity, or indium oxide without complete desorption from nature oxide. Therefore, it is reasonable that the sample B with more residual metal impurities and particles, thicker nature oxide thickness and rich indium surface has more defects density.

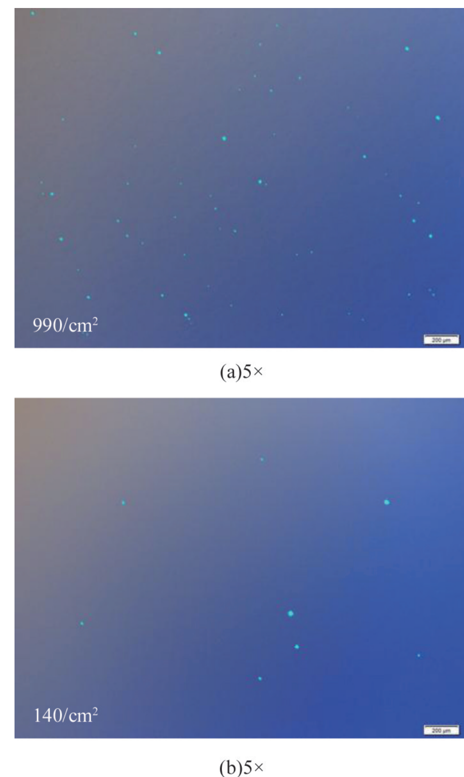

Fig. 3　Normarski microscope (a) sample B, and (b) sample C
图3　Normarski显微图片 (a)样品B,(b)样品C

3　Conclusion

HCl-based solution, combined with SC1 is beneficial for the reduction of particles and metals on InAs wafer surface. Lower concentration of H_2O_2 in the NH_4OH mixture produces thinner oxide and arsenic-rich oxide surface. InAs wafer with thin oxide and arsenic-rich oxide surface is good to high quality epitaxial growth. The

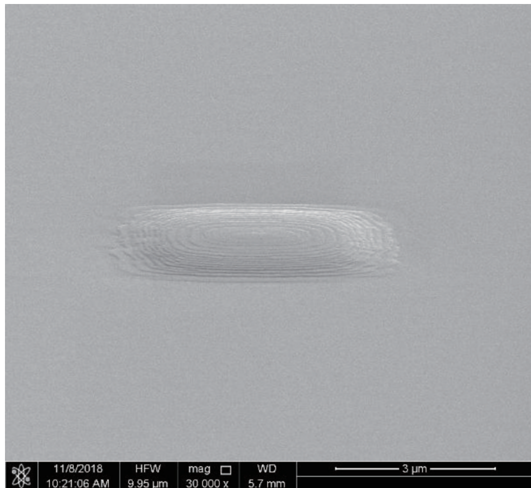

Fig. 4 Hillocks defect from scanning electron microscopy after SL growth
图4 生长InAs/GaSb超晶格后扫描电镜下小丘状缺陷

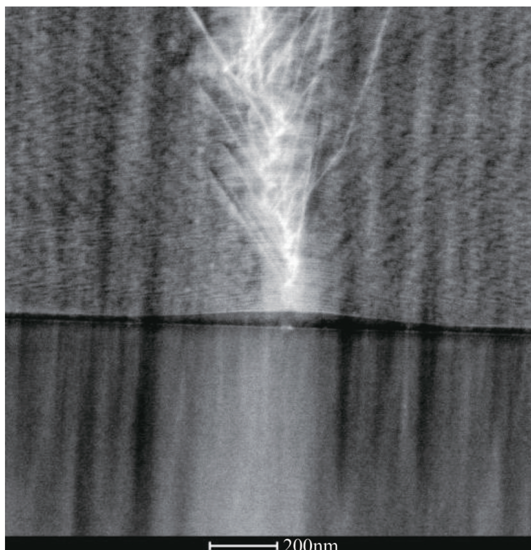

Fig. 5 Transmission electron microscope of hillocks defect
图5 透射电镜下小丘状缺陷成因

lower defect density of $140/cm^2$ from SL by MOCVD is obtained through InAs substrate treatment technique.

Acknowledgment

The authors gratefully acknowledge the support of the National Natural Science Foundation of China (Grant No. 61904175). The authors also gratefully acknowledge the Suzhou Institute of Nano-Tech and Nano-Bionics, Chinese Academy of Sciences for MOCVD and device fabrication process.

References

[1] Oda O. *Compound semiconductor bulk materials and characterizations* [M]. world scientific, 2007, p:331.

[2] Ning D D, Chen Y N, Li X K, *et al*. Research on the photoluminescence of spectral broadening by rapid thermal annealing on InAs/GaAs quantum dots[J]. *J. Semicond.*, 2020, **41**(12): 122101.

[3] Kroemer H. The 6.1 family (InAs, GaSb, AlSb) and its heterostructures: A selective review[J]. *Physica E Low-Dimensional Systems and Nanostructures*, 2004, **20**(3-4):196-203.

[4] Lee H J, Ko S Y, Kim Y H, *et al*. Strain-induced the dark current characteristics in InAs/GaSb type-II superlattice for mid-wave detector[J]. *J. Semicond.*, 2020, **41**(6): 062302.

[5] Yu T, Liu S M, Zhang J C, *et al*. InAs-based interband cascade lasers at 4.0 μm operating at room temperature[J]. *J. Semicond.*, 2018, **39**(11): 114003.

[6] Reinhardt K. Handbook of Silicon Wafer Cleaning Technology, 2nd Edition[M]/Handbook of silicon wafer cleaning technology

[7] Song J S, Choi Y C, Seo S H, *et al*. Wet chemical cleaning process of GaAs substrate for ready-to-use[J]. *Journal of Crystal Growth*, 2004, **264**(1/3):98-103.

[8] Sun Y, Liu Z, Machuca F, *et al*. Optimized cleaning method for producing device quality InP(100) surfaces[J]. *Journal of Applied Physics*, 2005, **97**(12):238-L667.

[9] Guivarc'h A, L'Haridon H, Pelous G, *et al*. Chemical cleaning of InP surfaces: Oxide composition and electrical properties[J]. *Journal of Applied Physics*, 1984, **55**(4):1139-1148.

[10] Liu Z, Sun Y , Machuca F, *et al*. Optimization and characterization of III - V surface cleaning[J]. *Journal of Vacuum ence & Technology B Microelectronics & Nanometer Structures*, 2003, **21**(21):184-187.

[11] L'Vova T V , Sedova I V , Dunaevski M S , *et al*. Sulfide passivation of InAs(100) substrates in Na2S solutions[J]. *Physics of the Solid State*, 2009, **51**(6):1114-1120.

[12] Losurdo M, Giangregorio M, *et al*. InAs(100) surfaces cleaning by an As-free low-temperature 100\\u00b0C treatment[J]. *Journal of The Electrochemical Society*, 2009, **156**(4):H263.

[13] Van Dorp D H, Arnauts S, Holsteyns F, *et al*. Wet-Chemical Approaches for Atomic Layer Etching of Semiconductors: Surface Chemistry, Oxide Removal and Reoxidation of InAs (100)[J]. *Ecs Journal of Solid State Science & Technology*, 2015, **4**(6):N5061-N5066.

[14] Yang L, Tan B M, Liu Y L, *et al*. Optimization of cleaning process parameters to remove abrasive particles in post-Cu CMP cleaning [J]. *J. Semicond.*, 2018, **39**(12):126002.

[15] Yang J, Lu W, Duan M L, *et al*. VGF growth of high quality InAs single crystals with low dislocation density[J]. *Journal of Crystal Growth*,2019, **531**:125350.

[16] Shen G, Zhao Y, Sun J, *et al*. A comparison of defects between InAs single crystals grown by LEC and VGF methods[J]. *Journal of Electronic Materials*, 2020, **49**:5104-5109.

[17] Lu X, Zhao Y, Sun W, *et al*. Lattice perfection of GaSb and InAs single crystal substrate[J]. *Pan Tao Ti Hsueh Pao/Chinese Journal of Semiconductors*, 2007, **28**(S1):163-166.

[18] Sun J, Shen G Y, Xie H, *et al*. Wet etching generation of dislocation pits with clear facets in LEC-InAs single crystals[J]. *Journal of Crystal Growth*, 2019, **526**:125237.

[19] Reinhardt K A. Handbook of silicon wafer cleaning technology[M]. third edtion.2018 Elsevier Inc. Applied science publishers.

[20] WU Jia, XU Zhi-cheng, Chen JX, *et al*. Wet etching for InAs-based InAs/Ga(As)Sb superlattice long wavelength infrared detectors [J]. *Journal of Infrared and Millimeter Waves*(吴佳,徐志成,陈建新,等。InAs基InAs/Ga(As)Sb II类超晶格长波红外探测器湿法腐蚀研究。**红外与毫米波学报**),2019, **38**(5):549-553.

[21] Liu F, Zhang L D, Liu H, *et al*. Characterization study of native oxides on GaAs(100) surface by XPS[C]// International Symposium on Photoelectronic Detection & Imaging. International Society for Optics and Photonics, 2013.

[22] Teng Y, Zhao Y, Wu Q H, *et al*. High performance long-wavelength InAs/GaSb superlattice detectors grown by MOCVD[J]. *IEEE Photonic Technology Letters*, 2019, **31**(2):185-188.